IHJPAS. 36 (4) 2023

Ibn Al-Haitham Journal for Pure and Applied Sciences
Journal homepage: jih.uobaghdad.edu.iq

Synthesis, Characterization and Surface Properties of Nano-TiO_2 Using a Novel Leaf Extracts

Rasha Tariq salim *
Department of Chemistry, College of Science,
University of Baghdad,Baghdad Iraq.

Dunya Edan AL-Mammar
Department of Chemistry, College of Science,
University of Baghdad,Baghdad Iraq.

***Corresponding Author: rashatariq46@gmail.com**

Article history: Received 26 December 2022, Accepted 22 January 2023, Published in October 2023.

doi.org/10.30526/36.4.3161

Abstract

The main focus of research is on the nature of applications in the fields of science and technology, particularly nanotechnology. In this paper, a simple, non-toxic, inexpensive, and environmentally friendly green method was used to synthesize TiO_2 nanoparticles using the extraction of portulacaria afra plant leaves and $TiCl_4$ as a precursor. The synthesized titanium dioxide nanoparticles were characterized by scanning electron microscopy, atomic force microscopy, X-ray diffraction patterns, Fourier transform infrared spectroscopy, and Brunauer-Emmett-Teller analysis. The SEM image of TiO_2 nanoparticles showed a few spherical, non-agglomerated particles. The average diameter of the nanoparticles, according to the surface topography of TiO_2-NPs, is 70.24 nm. It was found that the average crystalline size was 18.9 nm by utilizing the Debye-Scherrer equation to calculate the size of the crystals. The vibrational mode of Ti-O-Ti exhibits a distinctive peak in the broad band centered at 578.64, 547.78, and 514.99 cm^{-1}, which denotes the development of metal-oxygen bonding, confirming the presence of TiO_2-NPs. The specific surface of the synthesized particles was calculated using the Brunauer-Emmett-Teller BET equation.

Keywords: Green method, Portulacaria afra, Titanium dioxide nanoparticles, synthesized, Nanotechnology.

1. Introduction

Nanotechnology aims mainly to improve, develop, and utilize the unique properties of molecules at the nano level in order to enhance materials, instruments, and systems with fundamentally different properties. In all fields of science and technology, innovative ideas continued to be developed in the fields of medical technologies, sensor technology, energy resources, and environmental protection and preservation [1]. TiO_2 is a semiconductor material with a large band gap that can be crystalline as rutile, anatase, or brookite. It is a great material for chemical sensors, solar cells, photocatalysis, dye-sensitized solar cells, microelectronics,

electrochemistry, and charge-spreading devices [2]. The anatase phase of TiO2 nanocrystals has recently attracted attention due to their intriguing features as compared to the bulk and because they are essential not just for applications but also from a fundamental standpoint [3]. TiO_2-NPs can be synthesized chemically or physically using microwave [4], hydrothermal [5], solid state , solution route, sol gel [6], chemical phase breakdown vapor, solvothermal crystallization [7], co-precipitation [8], ultrasonic irradiation, and biologically applicable green synthesis methods [9].

Green synthesis is a simple process that utilizes a variety of biological agents, such as plants, bacteria, fungi, algae, and yeast, with no dangerous products [10]. Due to its low cost, simple technique, and scalability for large-scale production, green synthesis has greater advantages over physical and chemical processes. With this technique, expensive equipment, hazardous chemicals, high temperatures, and high pressure are not necessary [11]. As a result, plant and herbal extracts are more desirable due to the easier and more cost-effective process and the inclusion of compounds such as flavonoids, terpenoids, and polysaccharides [12]. The creation of environmentally safe nanoparticles with a variety of natural features, great stability, and suitable dimensions can be achieved through a one-step green reduction method called nano-TiO_2 biosynthesis for the production of biological nanoparticles [13]. TiO_2-NPs are created from a variety of plants, including the Jatropha curcas plant [14], the glycosmis cochinchinensis plant [15], the Syzygium cumini plant [16], the Moringa oleifera plant [17], the Psidium guajava plant [18], and the Aloe vera plant [11].

In this research, Portulacaria afra (PA) was used to synthesize TiO_2-NPs. (PA) is a succulent plant that is native to South Africa and can live in different regions of the world, including Iraq. (PA) is commonly found in semi-arid regions. This plant has small, succulent leaves and is in the form of a tall or small woody tree. The height of this plant can reach 2–5 meters. This plant contains bioactive substances such as alkaloids, amino acids, flavonoids, terpenoids, and other phenolic intermediates that may act as effective reducing agents for the bioreduction of metals into nanoparticles (NPs), which in turn have a variety of biological applications [19].

2. Materials and Methods

2.1. Materials

Titanium tetrachloride $TiCl_4$, 99.0% was purchased from CDH, Portulacaria afra leaves collected from a local garden in Baghdad, Iraq.

2.2. Methods

2.2.1. Biosynthesis of TiO_2-NPs by Portulacaria afra (PA)

In this method, TiO_2-NPs were synthesized using the aqueous extract of (PA) plant leaves. (PA) leaves were removed from the original plant, thoroughly cleaned with tap water to eliminate impurities, then rinsed with distilled water and chopped into little pieces. 25 g of chopped plant leaves were added to 100 mL of boiled distilled water and heated for two hours continuously at 90 ^oC.

The plant extract was filtered using a Whatman No. 1 filter solution. For the synthesis of titanium dioxide nanoparticles, 2.8 mL of titanium tetrachloride as an aprecursor was added to 100 mL of distilled water and shaken well. (PA) leaf extract was added to the titanium tetrachloride solution gradually with continuous stirring. The mixture was continually stirred for 4 hours. Titanium

dioxide nanoparticles were synthesized during this process, and they were separated by drying the precipitate for a day at room temperature. Then it was heated in an electric oven for one hour. The precipitate was dried for 24 hours at 100 ºC. Then the precipitate was calcined at 500 ºC for 4 hours continuously [11]. After that, the precipitate was often washed with distilled water to get rid of the impurities. To obtain titanium dioxide nanoparticles as a white precipitate, the precipitate was dried and heated at 700 ºC for one hour. Finally, a laboratory mill ground the precipitate and stored it for characterization and application. **Figure 1** shows the steps of TiO_2-NPs preparation from (PA) plant.

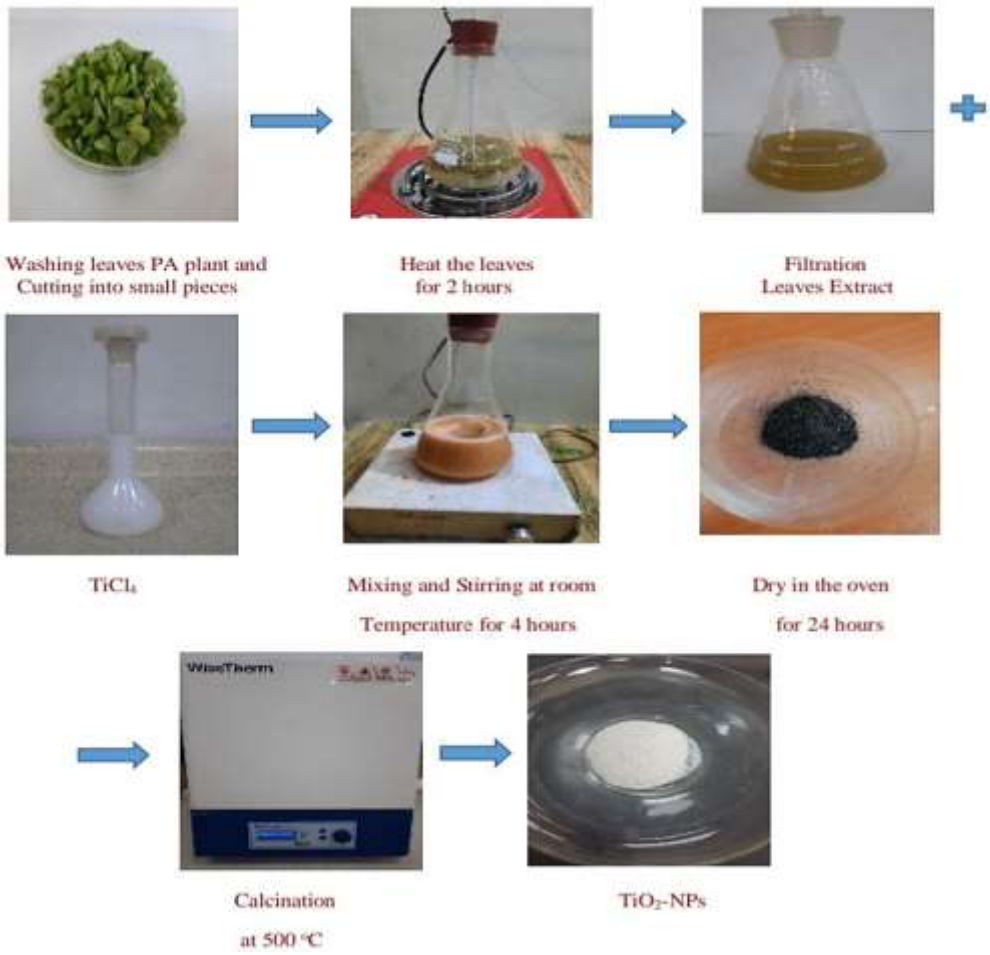

Figure 1. Steps of TiO_2-NPs preparation by (PA) plant.

2.2.2. Characterization of TiO_2-NPs

For chemical, structural, physical, and morphological evaluations, TiO_2 NPs were characterized. Analyses of the morphology of nano-TiO_2 were done using scanning electron microscopy (FESEM-EDS, MIRA III, TESCAN, and Czech). The physical assessment was done using atomic force microscopy (AFM 2022, Nanosurf, and Switzerland). Structural assessment of the nanoparticles was characterized using X-ray diffraction XRD (PW1730, Philips, and Holland). Chemical assessment was carried out using Shimadzu IR-Affinity-1 Japan. Brunauer-Emmett and Teller surface area analyzer type BELSORP MINI II, BEL, Japan, was applied to estimate the specific surface area, average pore volume, and pore size distribution [20] .These measurements were used to describe the topography and examine the characteristics of a material at the nanoscale.

3. Results and Discussion

3.1. Scanning Electron Microscopy (SEM)

SEM measurements were used to obtain the images of samples using the technique of scanning electron microscopy to explore the surface features, porosity morphology [21], and crystalline structure [22]. It can be seen from **Figure 2** that the sample showed excellent crystallinity. The particle size of TiO_2-NPs was 47.580 nm, which was calculated using IMAGE J software. The SEM image of TiO_2 nanoparticles revealed that TiO_2 has a nanosheet-like structure on its surface and is porous [23]. The SEM image showed that the TiO_2 nanoparticles had clumped together and took an irregular shape, which was obtained at a magnification of 500 nm. There were a few non-clumping particles that were spherical in shape. So, it can infer that the phytochemicals of Portulacaria afra leaf extract coat the surface of TiO_2 nanoparticles, inhibiting their accumulation [15].

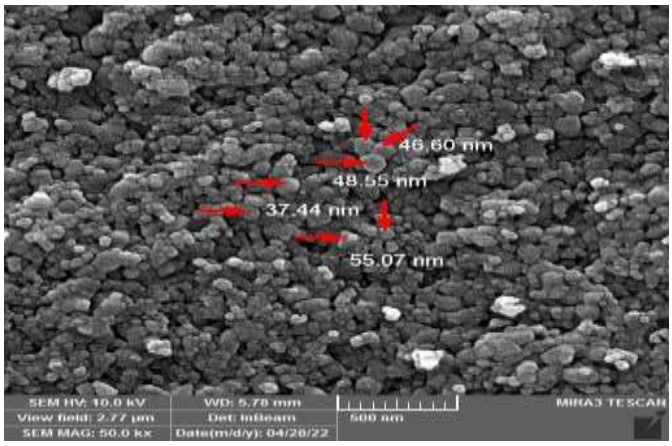

Figure 2. SEM image for TiO_2-NPs.

3.2. Atomic Force Microscopy (AFM)

AFM analysis is used to measure the important properties such as surface morphology with probes at nanometer scales [24]. The average diameter of prepared TiO_2-NPs is 70.24 nm. Through these results, it was observed that the sample that was synthesized by Green Biology produced a particle with a small size distribution. **Figures 3a, b** show the typical surface obtained from the AFM image and the granularity cumulating distribution for the TiO_2 sample.

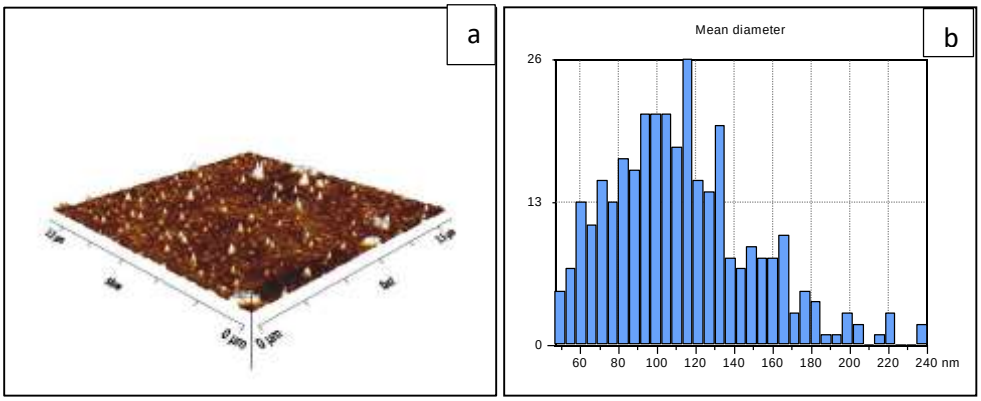

Figure 3 (a, b). View of AFM image and granularity cumulating distribution chart of TiO_2-NPs.

3.3. X-Ray Diffraction (XRD)

Figure 4 shows a polycrystalline structure of mixed anatase and rutile phases, which is how the crystalline structure of the synthesized TiO_2-NPs was explained by XRD patterns. The dominant Anatase phase angles 2θ= 25.5795°, 37.1949°, 38.0553°, 38.7313°, 48.2265°, 55.2019°, 62.8841°, 69.0913°, 70.5356°, 75.1449° correspond to crystalline planes (101), (103), (004), (112), (200), (211), (204), (116), (220), and (215), respectively, according to the standard card No. 96-152-6932. The diffraction peaks for the identified Rutile phase appeared at 27.6076°, 36.2423°, 41.5277°, 54.3108°, and 56.7998° corresponding to crystalline planes (110), (101), (111), (211), and (220), respectively, according to standard card No. 96-900-4142. The d_{hkl} value was calculated using Bragg law [25]:

$$n\lambda = 2\, d_{hkl} \sin\theta \qquad (1)$$

whereas the Debye-Scherrer equation was used to determine the value D [26]:

$$D = \frac{K\lambda}{\beta \cos\theta} \qquad (2)$$

Where D: crystallite size, K: constant Scherrer, λ: is the monochromatic wavelength of X-ray= 0.154061 nm, θ: diffraction angle, and β: full width at half maximum (FWHM) in rad. **Table 1** shows the X-ray peak parameters of TiO_2-NPs. The average crystalline size is 18.9 nm.

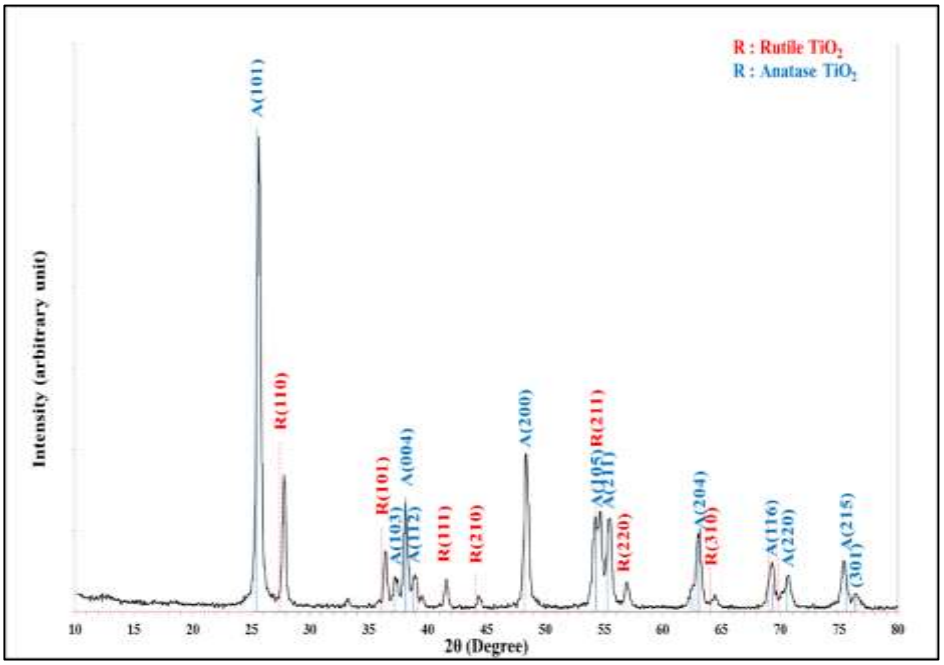

Figure 4. XRD pattern for TiO_2-NPs.

Table 1. XRD results for TiO_2-NPs.

2θ (Deg.)	FWHM (Deg.)	d_{hkl} (Å)	D (nm)	Phase
25.6218	0.3876	3.4740	21.0	AnataseTiO_2
27.7385	0.3279	3.2135	25.0	RutileTiO_2
36.3842	0.3876	2.4673	21.6	RutileTiO_2
37.2487	0.4472	2.4120	18.8	AnataseTiO_2
38.1133	0.4472	2.3592	18.8	AnataseTiO_2
38.8884	0.4174	2.3140	20.2	AnataseTiO_2
41.6312	0.4771	2.1677	17.8	RutileTiO_2
44.3739	0.4770	2.0398	18.0	RutileTiO_2
48.3986	0.4770	1.8792	18.3	AnataseTiO_2
54.2419	0.4770	1.6897	18.7	RutileTiO_2
54.6891	0.3875	1.6770	23.1	AnataseTiO_2
55.4940	0.4472	1.6545	20.1	AnataseTiO_2
56.8952	0.4472	1.6171	20.2	RutileTiO_2
63.1261	0.5367	1.4716	17.4	AnataseTiO_2
64.4080	0.5068	1.4454	18.5	RutileTiO_2
69.2973	0.6261	1.3549	15.4	AnataseTiO_2
70.6687	0.6559	1.3319	14.9	AnataseTiO_2
75.3790	0.5665	1.2599	17.7	AnataseTiO_2
76.3330	0.7752	1.2465	13.0	AnataseTiO_2

3.4. Fourier Transform Infrared Spectroscopy (FTIR)

FTIR spectra provide specific data about the chemical bonding and molecular structures of organic compounds and a limited number of inorganic materials. It is useful for the identification of unknown compounds when patterns of IR spectra are available. FTIR spectra were recorded over a wavelength range between 400 and 4000 cm^{-1}. **Figure 5** shows the FTIR spectrum of TiO_2-NPs. In this Figure, a wide absorption band at 3421.72 cm^{-1} is caused by the surface adsorbed moisture of the synthetic TiO_2-NPs straining the O-H bond. The weak absorption bands at 2380.16 and 2312.65 cm^{-1} could be caused by the C=O bond stretching generated by carbon dioxide that was adsorbed to the NPs surface .The O-H bending of water molecules was adsorbed on the particle surface, resulting in the absorption band appearing at 1627.92 cm^{-1}. The vibrational mode of Ti-O-Ti exhibits a distinctive peak in the broad band centered at 578.64, 547.78, and 514.99 cm^{-1}, which denotes the development of metal-oxygen bonding [27]. The peak at 2879.72, 2831.50 cm^{-1} confirmed the presence of secondary amines, and the peak at 1643.35 cm^{-1} was caused by the O-H bending vibration of adsorbed water molecules on the surface of TiO_2 which may play a significant role in photocatalytic activity. Strong peaks at 1546.91, 1531.48, and 1517.98 cm^{-1} indicate aliphatic nitro compounds with stretching of N-O [15].The peaks 1394.53, 1342.46, and 1319.31 cm^{-1} related to aliphatic amine-containing and C-N-stretched amines [28]. **Table 2** shows the FTIR spectrum data for TiO_2-NPs.

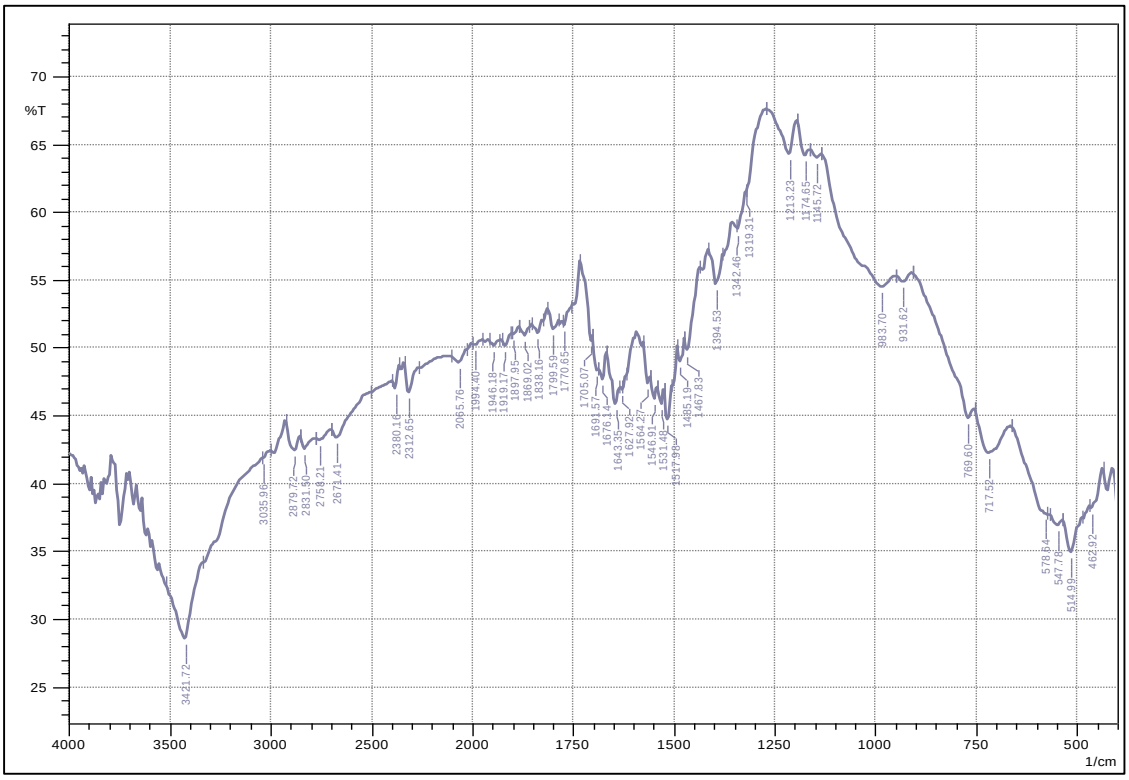

Figure 5. FTIR spectrum of TiO_2-NPs.

Table 2. FTIR spectrum data for TiO_2-NPs.

No.	Peak	Intensity	Corr. Intensity	Base (H)	Base (L)	Area	Corr. Area
1	462.92	38.136	0.701	468.7	435.91	13.37	0.219
2	514.99	34.965	2.411	536.21	487.99	21.27	0.667
3	547.78	36.898	0.535	569	536.21	14.067	0.097
4	578.64	37.787	0.304	663.51	574.79	34.63	0.18
5	717.52	42.249	2.759	754.17	663.51	32.932	1.389
6	769.6	44.835	1.693	908.47	754.17	46.266	0.189
7	931.62	54.851	0.54	948.98	908.47	10.472	0.085
8	983.7	54.489	2.49	1134.14	948.98	44.676	3.093
9	1145.72	64.023	0.402	1163.08	1134.14	5.558	0.04
10	1174.65	64.182	1.239	1193.94	1163.08	5.777	0.143
11	1213.23	64.245	2.742	1271.09	1193.94	13.885	0.567
12	1319.31	61.528	0.266	1321.24	1271.09	9.324	-0.218
13	1342.46	58.716	0.674	1346.31	1321.24	5.603	0.088
14	1394.53	54.728	2.34	1413.82	1379.1	8.776	0.324
15	1467.83	49.757	1.76	1473.62	1435.04	10.826	0.274
16	1485.19	48.966	1.392	1490.97	1473.62	5.294	0.137
17	1517.98	44.704	2.287	1523.76	1504.48	6.591	0.275
18	1531.48	45.865	1.131	1541.12	1523.76	5.788	0.097
19	1546.91	46.206	1.171	1558.48	1541.12	5.724	0.113
20	1564.27	47.42	1.336	1575.84	1558.48	5.468	0.115
21	1627.92	46.873	0.374	1629.85	1618.28	3.763	0.028
22	1643.35	45.841	1.887	1666.5	1635.64	10.038	0.302
23	1676.14	47.677	1.446	1687.71	1666.5	6.672	0.111
24	1691.57	48.291	0.847	1701.22	1687.71	4.175	0.068
25	1705.07	50.517	1.037	1732.08	1701.22	8.377	0.008
26	1770.65	51.663	0.586	1776.44	1755.22	5.965	0.025
27	1799.59	51.406	1.027	1813.09	1786.08	7.693	0.121
28	1838.16	51.096	0.826	1851.66	1826.59	7.234	0.094
29	1869.02	50.917	0.644	1884.45	1859.38	7.284	0.071
30	1897.95	50.976	0.193	1901.81	1884.45	5.052	0.022
31	1919.17	50.179	0.596	1926.89	1905.67	6.304	0.07
32	1946.18	50.163	0.4	1959.68	1934.6	7.47	0.045
33	1994.4	50.195	0.232	2002.11	1975.11	8.045	0.031

3.5. BET analysis

The characteristic and adsorption capacity of the synthesized TiO_2-NPs could be predicted from the surface area and porosity information obtained from the BET equation [29]. The specific surface area was calculated from the BET equation and found to be 14.741 m^2/g, as shown in **Figure 6**. The total pore volume and mean pore diameter were found to be equal to 0.1191 cm^3/g and 32.304 nm, respectively. The N_2 gas adsorption/desorption isotherm for TiO_2-NPs is presented in **Figure 7**. This figure shows the presence of a cylindrical pore in this sample with a narrow distribution of uniform pores [30].

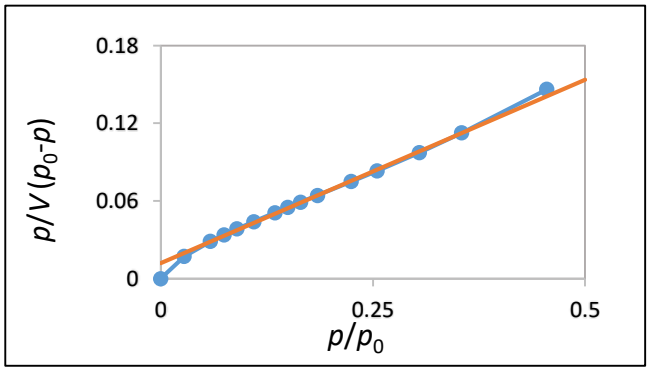

Figure 6. BET plot for N_2 gas adsorption isotherm at 77 K for TiO_2-NPs.

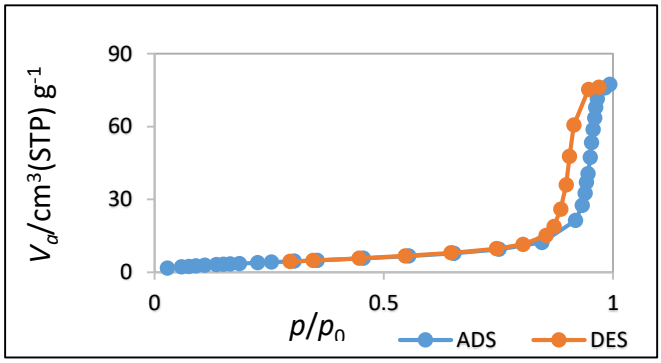

Figure 7. Nitrogen gas adsorption/desorption isotherm for TiO_2-NPs.

4. Conclusion

The environmentally friendly technique for producing TiO_2-NPs from PA plant extract compared to other preparation methods could be a promising technology because it uses no hazardous chemicals and is environmentally benign. SEM, AFM, XRD, FTIR, and BET are among the diagnostic methods used to describe the prepared particles. A few spherical, non-agglomerated particles could be seen in the SEM image of TiO_2 nanoparticles. When the surface topography of TiO_2-NPs was studied, an average diameter of 70.24 nm was observed. Through the use of Debye Scherrer, the crystallite size was calculated. The crystalline size was 18.9 nm on average. The presence of TiO_2-NPs is confirmed by the vibrational mode of Ti-O-Ti, which displays a characteristic peak in the broad band centered at 578.64, 547.78, and 514.99 cm^{-1}. This peak indicates the development of metal-oxygen bonding. According to BET analysis, the specific surface area was 14.741 m^2 / g and the total pore volume was 0.1191 cm^3 / g.
Titanium dioxide nanoparticles, especially those prepared by green methods, have many unique features and characteristics that enable them to be used to treat environmental pollution problems. For future work, it is recommended:

1. Study the use of the green synthesized TiO_2-NPs to get rid of other contaminants from the environment, such as heavy metals.
2. Study the possibility of using these prepared nanomaterials in medical

References

1. Hussain, C. M. ; Mishra, A. K. Nanotechnology for Sustainable Water Resources. *John Wiley & Sons* **2018**.
2. Dusastre, V. Materials for sustainable energy: A Collection of Peer-Reviewed Research and Review Articles from Nature Publishing Group. *World Scientific* **2010**.
3. Gao, L.; Zhang, Q. Effects of Amorphous Contents and Particle Size on the Photocatalytic Properties of TiO_2 Nanoparticles. Scripta materialia **2001**, *44*, 1195-1198.
4. Lee, H. B.; Choi, M. S.; Kye, Y. H.; An, M.Y.; Lee, I. M. Control of Particle Characteristics in the Preparation of TiO_2 Nano Particles Assisted by Microwave. Bulletin of the Korean Chemical Society **2012**, *33*, 1699-1702.
5. Shivaraju, H.; Byrappa, K.; Kumar, T.V.; Ranganathaiah, C. Hydrothermal Synthesis and Characterization of TiO_2 Nanostructures on the Ceramic Support and Their Photo-Catalysis Performance. *Bulletin of the Catalysis Society of India* **2010**, *9*, 37-50.

6. Thangavelu, K.; Annamalai, R.; Arulnandhi, D. Preparation and Characterization of Nanosized TiO_2 Powder by Sol-Gel Precipitation Route. *International Journal of Emerging Technology and Advanced Engineering* **2013**, *3*, 636-639.

7. Dinh, C. T.; Nguyen, T. D.; Kleitz, F.; Do, T.O. A Solvothermal Single-Step Route Towards Shape-Controlled Titanium Dioxide Nanocrystals. T*he Canadian Journal of Chemical Engineering* **2012**, *90*, 8-17.

8. Rasool, K.; Usman, M.; Ahmad, M.; Imran, Z.; Rafiq, M. A.; Hasan, M.M.; Nazir, A.Effect of Modifiers on Structural and Optical Properties of Titania (TiO_2) Nanoparticles. Saudi International Electronics, Communications and Photonics Conference (SIECPC) **2011**, 1-4.

9. Aravind, M.; Amalanathan, M.; Mary, M. Synthesis of TiO_2 Nanoparticles by Chemical and Green Synthesis Methods and Their Multifaceted Properties. *SN Applied Sciences* **2021**, *3*, 1-10.

10. Huq, M.A.; Ashrafudoulla, M.; Rahman, M.; Balusamy, S.R.; Akter, S. Green Synthesis and Potential Antibacterial Applications of Bioactive Silver Nanoparticles: A Review. Polymers ***2022***, *14*, 742.

11. Rao, K.G.; Ashok, C.; Rao, K.V.; Chakra, C.; Tambur, P. Green Synthesis of TiO_2 Nanoparticles Using Aloe Vera Extract. Int. J. *Adv. Res. Phys. Sci* **2015**, *2*, 28-34.

12. Alamdari, S.; Sasani Ghamsari, M.; Lee, C.; Han, W.; Park, H. H.; Tafreshi, M. J.; Ara, M.H.M. Preparation and Characterization of Zinc Oxide Nanoparticles Using Leaf Extract of Sambucus Ebulus. Applied Sciences **2020**, *10*, 3620.

13. Abu-Dalo, M.; Jaradat, A.; Albiss, B.A.; Al-Rawashdeh, N. A. Green Synthesis of TiO_2 NPs/Pristine Pomegranate Peel Extract Nanocomposite and Its Antimicrobial Activity for Water Disinfection. *Journal of Environmental Chemical Engineering* **2019**, *7*, 103370.

14. Goutam, S. P.; Saxena, G.; Singh, V.; Yadav, A. K.; Bharagava, R. N.; Thapa, K. B. Green Synthesis of TiO_2 Nanoparticles Using Leaf Extract of Jatropha Curcas L. for Photocatalytic Degradation of Tannery Wastewater. *Chemical Engineering Journal* **2018**, *336*, 386-396.

15. Rosi, H.; Kalyanasundaram, S. Synthesis, Characterization, Structural and Optical Properties of Titanium-Dioxide Nanoparticles Using Glycosmis Cochinchinensis Leaf Extract and Its Photocatalytic Evaluation and Antimicrobial Properties. *World News of Natural Sciences* **2018**, *17*.

16. Sethy, N.K.; Arif, Z.; Mishra, P.K.; Kumar, P. Green Synthesis of TiO_2 Nanoparticles from Syzygium Cumini Extract for Photo-catalytic Removal of Lead (Pb) in Explosive Industrial Wastewater. *Green Processing and Synthesi*s **2020**, *9*, 171-181.

17. Patidar, V.; Jain, P. Green Synthesis of TiO_2 Nanoparticle Using Moringa Oleifera Leaf Extract. *Int Res J Eng Technol* **2017**, *4*, 1-4.

18. Santhoshkumar, T.; Rahuman, A. A.; Jayaseelan, C.; Rajakumar, G.; Marimuthu, S.; Kirthi, A. V.; Kim, S. K. Green Synthesis of Titanium Dioxide Nanoparticles Using Psidium Guajava Extract and Its Antibacterial and Antioxidant Properties. Asian Pacific *journal of tropical medicine* **2014**, *7*, 968-976.

19. A Salaheldin, T.; A El-Chaghaby, G.; A El-Sherbiny, M. Green Synthesis of Silver Nanoparticles Using Portulacaria Afra Plant Extract: Characterization and Evaluation of Its Antibacterial, Anticancer Activities. *Novel Research in Microbiology Journal* **2019**, *3*, 215-222.

20. Kareem, S.H.; Al-Hussien, E. Adsorption of Congo, Red Rhodamine B and Disperse Blue Dyes from Aqueous Solution Onto Raw Flint Clay. *Baghdad Sci J* **2012**, *9*, 680-688.

21. Supriya, S.; Sathish, S. Enhanced Photocatalytic Decolorization of Congo Red Dye with Surface-Modified Zinc Oxide Using Copper (II)-Amino Acid complex. *Inorganic and nano-metal chemistry* **2020**, *50*, 100-109.

22. Saed, S.A.; AL-Mammar, D.E. Influence of Acid Activation of a Mixture of Illite, Koalinite, and Chlorite Clays on the Adsorption of Methyl Violet 6B Dye. *Iraqi Journal of Science* **2021**, 1761-1778.

23. Rahimi, R.; Parvaz, S.; Rabbani, M. Adsorption of methyl orange by zinc oxide synthesized via a facile precipitation method. *MDPI AG* **2017.**

24. Rajeshkumar, S.; Santhoshkumar, J.; Jule, L. T.; Ramaswamy, K. Phytosynthesis of Titanium Dioxide Nanoparticles Using King of Bitter Andrographis Paniculata and Its Embryonic Toxicology Evaluation and Biomedical Potential. Bioinorganic Chemistry and Applications **2021**.

25. Kadhim, H.H.; Saleh, K.A. Removing of Copper Ions from Industrial Wastewater Using Graphene oxide/Chitosan Nanocomposite. *Iraqi Journal of Science* **2022** 1894-1908.

26. Al-Saadi, T. M. Investigating the Structural and Magnetic Properties of Nickel Oxide Nanoparticles Prepared by Precipitation Method. *Ibn AL-Haitham Journal For Pure and Applied Science*s **2022**, *35*, 94-103.

27. Tilahun Bekele, E.; Gonfa, B. A.; Sabir, F. K. Use of Different Natural Products to Control Growth of Titanium Oxide Nanoparticles in Green Solvent Emulsion, Characterization, and Their Photocatalytic Application. Bioinorganic Chemistry and Applications **2021**.

28. Narayanan, M.; Vigneshwari, P.; Natarajan, D.; Kandasamy, S.; Alsehli, M.; Elfasakhany, A.; Pugazhendhi, A. Synthesis and Characterization of TiO_2 NPs by Aqueous Leaf Extract of Coleus Aromaticus and Assess Their Antibacterial, Larvicidal, and Anticancer Potential. *Environmental Research* **2021**, *200*, 111335.

29. Zafar, M.N.; Dar, Q.; Nawaz, F.; Zafar, M.N.; Iqbal, M.; Nazar, M.F. Effective Adsorptive Removal of Azo Dyes Over Spherical ZnO Nanoparticles. *Journal of Materials Research and Technology* **2019**, *8*, 713-725.

30. Ho, Y. S. Second-Order Kinetic Model for the Sorption of Cadmium onto Tree Fern: A Comparison of Linear and Non-linear Methods. *Water research* **2006**, *40*, 119-125.